THE ASTRONOMICAL JOURNAL VOLUME 88, NUMBER 7 JULY 1983

PROPER MOTIONS OF HERBIG-HARO OBJECTS. III. HH-7 THROUGH -11, HH-12, AND HH-32[a]

G. H. HERBIG AND B. F. JONES
Lick Observatory, Board of Studies in Astronomy and Astrophysics, University of California, Santa Cruz, California 95064
Received 18 February 1983; revised 28 March 1983

ABSTRACT

Proper motions have been measured on Crossley and 120-in. plates for additional Herbig-Haro Objects. The bright, nearly stellar HH-11 shows definite motion away from the heavily obscured H_2O maser and infrared source SSV-13, about 16″ distant. Three other nearby Objects show no detectable motions. Repetitive ejection from the vicinity of SSV-13 at intervals of > 500 years is suggested. Nuclei in the nearby extended object HH-12 show motion away from another obscured star, SSV-11, of type Mleα. The indicated travel time is 800–1400 years. All these Objects have negative radial velocities with respect to the molecular cloud, and lie in regions of negative CO velocity. No Objects have been found on the opposite sides of the exciting stars, where the velocity would presumably be positive. HH-32A, B are moving away from the bright T Tauri star AS-353A, and have both large positive velocities and double emission lines. The line splitting is interpreted in terms of pre- and post-shock gas on the front side of an (invisible) obstacle in the wind from AS-353A.

I. INTRODUCTION

This is the third in the current series of papers (I: Herbig and Jones 1981; II: Jones and Herbig 1982) on the proper motions of Herbig-Haro Objects. These investigations have been possible because of the existence of early Lick direct plates of H-H fields taken at the prime foci of the Crossley reflector (scale: 39″ mm^{-1}) since 1946 and the 120-in. reflector (13″ mm^{-1}) since 1959, supplemented on occasion by early photographs from other sources. In this paper, the astrometric procedures and results are given in Sec. II, the distances are considered in Sec. III, and the discussions of individual fields appear in Sec. IV (HH-7 through -11), Sec. V (HH-12), and Sec. VI (HH-32). The identifications and numbering are those of Herbig (1974).

II. ASTROMETRY

a) NGC 1333

The individual H-H Objects in the region of NGC 1333 range in appearance from the nearly stellar (HH-11) to the large diffuse collection making up HH-12. Some of the knots are easily measurable (HH-11), while others are difficult even on the best plates. We had available for measurement four plates taken with the Lick 120-in. reflector as well as six plates taken with the Lick 36-in. Crossley reflector, all in red light. The details are given in Table I.

Sixty-three stars in the region of NGC 1333 were measured on these plates with the Lick Automatic Measuring Engine. The H-H Objects were hand measured on the Gaertner one-coordinate machine at Lick, along with a selection of reference stars used to reduce the hand measures to the AME system. Only the brighter H-H Objects could be measured on the Crossley plates (HH-11 and the brighter knots of HH-12).

The reduction procedure for the proper motions was similar to that described in Papers I and II: an iterative central plate overlap algorithm was used (Eichhorn and Jefferies 1971), and the radial distortion was removed with the same model as before, using plate ED-30, taken without the Ross corrector, as the standard plate. The errors of the stellar proper motions ranged from 0.″1 $cent^{-1}$ to 0.″9 $cent^{-1}$ depending on the magnitude and the number of plates on which the star appeared. Several of the H-H Objects could only be measured on the first 120-in. plate (ED-30) and the two most recent 120-in. plates (ED-2800 and ED-2850). This made the proper motion error determination for these objects rather uncertain, since there was no check on positional errors on the one first-epoch plate. We have increased the computed errors for these proper motion determinations by assuming that the positional errors at the first epoch

TABLE I. Plates.

Plate	Epoch (1900. +)	Exp (min)	Emulsion	Filter	Field
ED-30	59.93	50	103a-E	RG-1	NGC 1333
ED-2796	77.59	40	103a-E	RG-1	NGC 1333
ED-2800	80.79	50	103a-E	RG-1	NGC 1333
ED-2850	81.84	60	103a-E	RG-1	NGC 1333
CD-429	56.91	60	103a-E	RG-1	NGC 1333
CD-480	57.73	50	103a-E	RG-1	NGC 1333
CD-602	59.86	50	103a-E	RG-1	NGC 1333
CD-3099	81.00	60	103a-E	RG-1	NGC 1333
CD-3227	81.83	60	103a-E	RG-1	NGC 1333
CD-3231	81.91	60	103a-E	RG-1	NGC 1333
ED-1802	63.50	60	103a-E	RG-1	HH-32
ED-2298	70.68	60	103a-E	RG-1	HH-32
ED-2797	80.79	43	103a-E	RG-1	HH-32

[a] Lick Observatory Bulletin 962.

0004-6256/83/071040-13$00.90

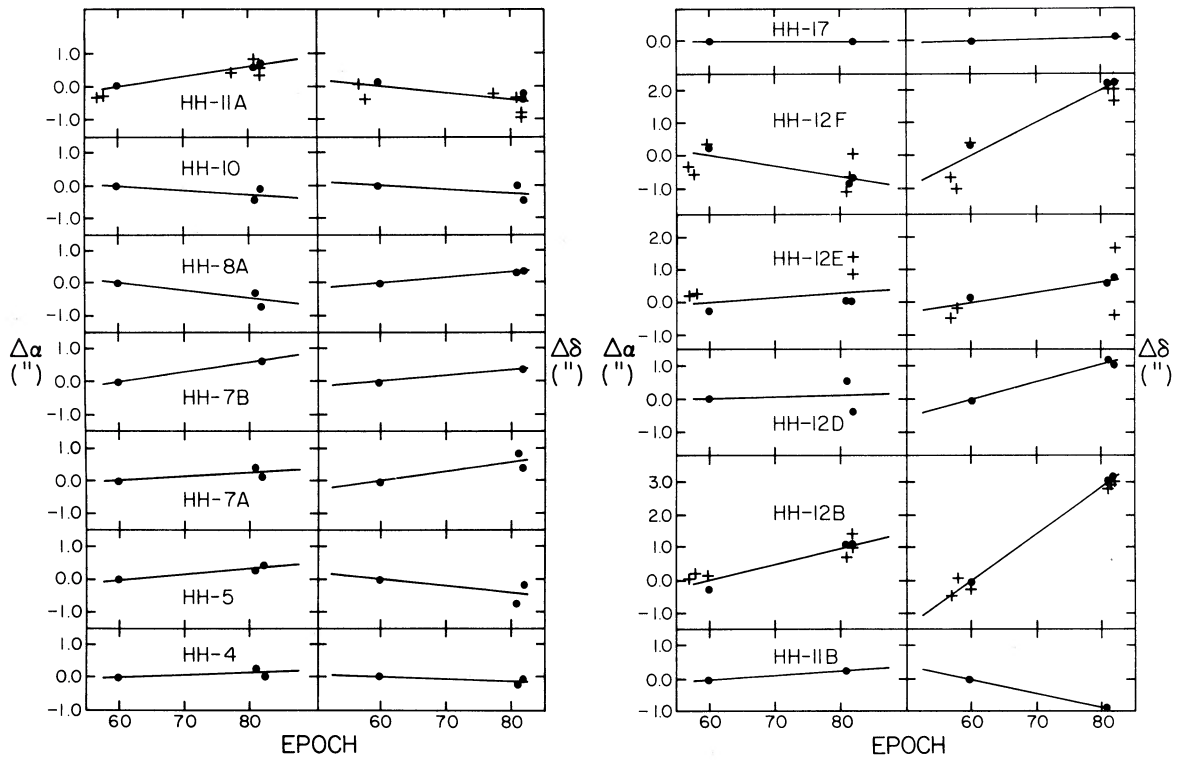

FIG. 1. The positional changes of the H-H Objects in the region of NGC 1333, in right ascension (left panels) and declination (right panels) as a function of time. Closed circles represent 120-in. measures and crosses Crossley measures. The straight lines are the least-squares proper motion fits to the points.

were of the same size as those of the second-epoch plates. The proper motions determined here are relative to the mean motion of the stars likely to be associated with NGC 1333 (i.e., projected upon the heavy obscuration around NGC 1333). As is shown below, these stars have a small dispersion in proper motion, although their absolute motion could be fairly large. Figure 1 shows the motions of each of the knots measured.

Figure 2 shows the proper motion vector diagram for the stars measured. The direction corresponding to motion towards the Solar antapex is shown as an arrow, with the length of the arrow corresponding to the reflex solar motion at a distance of 200 pc. The closed circles are stars projected upon heavy obscuration, while the open circles are stars near the edge of the cloud. Most of the stars projected upon the obscuration are not foreground stars, since they show a dispersion in proper motion that can be accounted for by the proper motion errors. These stars are most likely dynamically associated with the cloud. The stars near the edge of the obscuration show a much larger dispersion in proper motion.

Positions were determined for the H-H Objects and measured stars by first setting up a secondary reference frame of faint stars. The positions of these faint stars were determined using AGK3 stars in the region of NGC 1333 measured on a Lick 20-in. Carnegie Astrograph plate, AY-7950. This secondary reference frame was then used with the measures from the 120-in. and

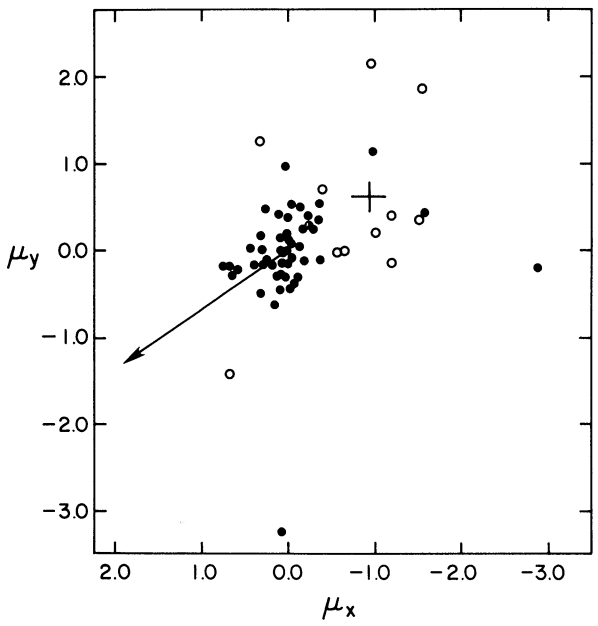

FIG. 2. The proper motion vector diagram for stars in region of NGC 1333. The closed circles are stars projected upon heavy obscuration, while the open circles are stars near the edge of the obscuration. The tip of the arrow represents the effect of the reflex solar motion at a distance of 200 pc. The large cross represents the absolute zero of the proper motion system assuming the motion of NGC 1333 is entirely due to reflex solar motion.

TABLE II. HH Objects near NGC 1333.

	α (1950)	δ	μ_x	σ_x	μ_y	σ_y	Telescope
HH-4	$3^h26^m18^s35$	31° 9′40″3	0.8	2.0	−0.6	2.0	120-in.
HH-5	3 26 14.72	31 2 32.8	1.8	2.0	−2.1	2.5	120-in.
HH-7a	3 26 2.76	31 5 10.2	1.4	2.0	2.9	2.0	120-in.
HH-7b	3 26 2.51	31 5 9.7	3.0	2.1	1.9	2.1	120-in.
HH-8a	3 26 0.72	31 5 18.3	−2.2	2.0	1.7	2.0	120-in.
HH-10	3 25 59.85	31 5 29.4	−1.1	2.0	−1.0	2.0	120-in.
HH-11a	3 25 59.00	31 5 35.1	3.0	0.5	−1.8	0.8	120-in., Crossley
HH-11b	3 25 58.97	31 5 34.1	1.4	2.1	−4.3	2.1	120-in.
HH-12b	3 25 53.44	31 10 9.8	5.0	0.7	14.4	0.6	120-in., Crossley
HH-12d	3 25 52.38	31 9 49.9	0.5	3.8	5.5	2.0	120-in.
HH-12e	3 25 53.66	31 9 47.9	1.5	1.7	3.2	1.7	120-in., Crossley
HH-12f	3 25 53.78	31 9 28.3	−3.1	1.2	10.2	1.1	120-in., Crossley
HH-17	3 26 14.74	31 8 16.4	0.0	2.1	0.7	2.1	120-in.

Crossley plates to determine the positions for all stars and the H-H Objects. Positions are for an equator and equinox of 1950.0 and an epoch of 1959.9. Table II gives the positions and proper motions for the H-H Objects and Table III gives the same data for the stars.

b) AS-353 A and B and HH-32

The knots of HH-32 are diffuse and not easy to measure. HH-32B and -32D are also faint. We had available only the three 120-in. plates listed in Table I, all taken in red light. The images of AS-353A and B were overexposed on these plates, making them also difficult to measure. The knots of HH-32 and AS-353A and B were hand measured on the Gaertner one-coordinate machine, along with a selection of reference stars. Three hundred field stars were measured on the AME. The hand measures of the selected reference stars were used to reduce the hand measures of AS-353A and B and the knots of HH-32 to the system of the AME.

The measures were reduced in a similar manner to those of the region of NGC 1333. The only difference was that in this case all plates were taken with the Ross corrector. We used mean distortion coefficients to cor-

TABLE III. Stars near NGC 1333.

No.	α (1950)	δ	μ_x	μ_y	No.	α (1950)	δ	μ_x	μ_y
1	$3^h26^m23^s57$	31° 8′17″4	0.2	0.3	33	$3^h25^m45^s49$	31° 6′13″2	0.1	−0.3
2	3 26 17.42	31 10 12.8	0.0	−0.5	34	3 25 47.33	31 6 7.3	−0.0	−0.0
3	3 26 11.05	31 6 0.8	−0.1	0.1	35	3 25 49.48	31 6 9.7	0.1	−0.3
4	3 25 54.77	31 3 19.9	−0.4	−0.1	36	3 25 49.55	31 6 5.8	−0.0	−0.3
5	3 25 46.91	31 5 7.1	−1.6	0.5	37	3 25 48.49	31 6 35.1	0.0	−0.0
6	3 25 57.28	31 5 42.3	0.3	0.0	38	3 25 49.02	31 6 32.0	−0.0	−0.0
7	3 25 52.47	31 7 44.7	0.2	−0.1	39	3 25 51.35	31 6 3.3	0.4	0.0
8	3 25 53.86	31 11 27.7	−0.1	−0.3	40	3 25 56.55	31 5 52.6	0.1	0.2
9	3 25 45.57	31 9 35.2	−0.2	0.3	42	3 25 46.57	31 5 27.9	−0.3	0.3
10	3 26 4.13	30 58 50.6	0.0	0.4	43	3 26 6.93	31 4 38.5	−2.9	−0.2
11	3 25 58.15	31 11 29.8	−0.4	0.4	45	3 26 1.93	31 0 29.8	−1.0	2.1
12	3 25 57.41	31 12 19.3	−0.2	0.4	46	3 26 16.26	31 5 18.4	−0.2	0.2
13	3 26 2.20	31 12 33.0	−0.1	0.5	47	3 26 15.82	31 5 37.1	−1.0	1.1
14	3 26 3.88	31 12 38.2	0.1	−0.5	48	3 26 22.51	31 6 11.2	0.7	−0.2
15	3 26 7.36	31 12 34.8	−0.0	0.1	49	3 26 24.68	31 8 46.2	0.0	0.0
16	3 26 7.12	31 13 11.3	0.2	−0.1	50	3 26 28.69	31 8 53.3	0.3	1.3
17	3 26 15.81	31 10 52.8	0.0	0.2	51	3 26 28.63	31 7 26.4	−0.1	−0.0
18	3 25 54.69	31 10 26.7	0.2	−0.2	52	3 26 21.85	31 10 53.5	0.0	−3.2
19	3 25 51.77	31 9 31.4	−0.1	−0.4	53	3 26 24.01	31 10 45.6	0.1	−0.1
20	3 25 52.03	31 9 28.9	0.1	0.0	100	3 26 16.22	31 13 58.0	0.6	−0.3
21	3 25 51.01	31 8 16.4	−0.2	−0.1	101	3 26 17.68	31 13 13.6	0.7	−0.2
22	3 25 50.62	31 7 26.6	−0.1	0.0	102	3 26 12.94	31 13 7.6	0.3	0.5
23	3 25 58.44	31 6 48.7	−0.1	0.4	103	3 26 11.90	31 12 27.0	−0.0	1.0
24	3 25 42.59	31 9 3.5	−0.1	0.5	104	3 26 25.06	31 13 35.7	−1.6	1.8
25	3 25 41.24	31 10 8.1	0.3	−0.5	105	3 26 26.70	31 14 20.1	−0.4	0.5
26	3 25 37.99	31 7 16.7	−0.1	−0.1	106	3 26 14.55	30 59 36.3	−1.2	0.4
27	3 25 37.69	31 7 13.2	0.0	0.0	107	3 26 13.19	30 59 41.4	−1.6	0.4
28	3 25 31.39	31 7 15.3	−0.6	0.0	108	3 26 9.42	30 59 9.3	−0.7	0.1
29	3 25 30.95	31 9 8.7	0.4	−0.2	109	3 25 46.47	31 12 25.7	0.5	−0.2
30	3 25 40.62	31 6 19.0	0.0	−0.2	110	3 25 31.31	31 12 51.7	0.6	−1.4
31	3 25 40.53	31 6 25.0	0.1	−0.7	111	3 25 33.99	31 11 37.0	−1.2	−0.2
32	3 25 42.25	31 6 35.5	−0.4	0.7					

TABLE IV. HH-32 and AS-353A, B.

	α (1950)	δ	μ_x	σ_x	μ_y	σ_y
AS-353A	$19^h\,18^m\,9^s.41$	10°56′14″.8	−0.6	1.0	−0.8	1.0
AS-353B	19 18 9.45	10 56 9.1	0.5	1.0	−1.1	1.0
HH-32A	19 18 7.94	10 56 21.6	−3.8	2.1	0.6	1.5
HH-32B	19 18 8.29	10 56 16.6	−13.2	2.5	5.1	1.5
HH-32D	19 18 9.71	10 56 10.6	−0.3	1.5	−1.8	1.5

rect the measures of plate ED-2298, and reduced the other plates to this system. The proper motions determined here are relative to field stars that are largely background to the cloud containing AS-353. Positions were determined in the same manner as for the region of NGC 1333, using plate AY-8249 to set up the secondary reference frame. The positions are for an equator and equinox of 1950.0 and an epoch of 1970.68. The positions and proper motions are given in Table IV, while Fig. 3 shows the motions for each of the knots as well as for AS-353A and B.

III. DISTANCES

a) NGC 1333 and HH-7 through HH-12

The distance of 500 pc is usually assigned to the reflection nebula NGC 1333, which is the portion of the dark cloud B205 illuminated by BD + 30°549. This distance is based on the B, V magnitudes and the B9 V type assigned to the star by Strom, Grasdalen, and Strom (1974). Unpublished photometry of + 30°549 by J. Smak with the Crossley reflector on two nights in 1962 yielded $V = 10.56$, $B - V = 0.50$, $U - B = -0.09$, values which translate to B5 V on a reddening line of conventional slope and correspond to a distance of 800 pc if one assumes Blaauw's (1963) value of $M_V = -1.0$ for B5 V. Smak's photometry, like that of Strom *et al.* leads to 500 pc if the star is taken to be a normal B9 V. Both of these results are in conflict with the following information. (1) The small cluster IC 348 is embedded in the dark cloud B4, which is clearly linked (through B1) with B205. The well-determined distance of IC 348, from four early-type members, is 380 pc (Harris, Morgan, and Roman 1954). (2) IC 348 belongs to the Per OB2 association, for which Borgman and Blaauw (1964) have determined a distance of 330 pc from the colors and magnitudes of 14 bright B-type members. (3) The nebulous star HD 21110 illuminates part of B205. An MK type of K3 III was assigned by Herbig. The UBV photometry of Cohen (1975), the assumption of normal reddening, and Blaauw's $M_V = +0.1$ for K3 III leads to a distance of 190 pc. This result hinges upon the correctness of the spectroscopic luminosity classification. For example, if the star were really of class II-III, which is within the uncertainty of the classification, the distance would be 380 pc. Thus although the spectroscopic luminosity of HD 21110 is too uncertain to confirm the value from (1) and (2), above, it is not incompatible with them. A distance of about 350 pc for NGC 1333 and B205 could be reconciled with Smak's photometry of + 30°549 if the appropriate value of $A_V/E\,(B - V)$ for NGC 1333 were 4–6 rather than the normal 3.1. This would not be surprising, because large values of A/E are often reported for dense dark clouds. In the absence of other information, one should not employ + 30°549 for determination of the distance. Furthermore, inspection of direct photographs does not persuade us of a connection between these dark nebulae and the Taurus clouds, to the south and east. On that account we do not favor the suggestion of Young, Goldsmith, Langer, Wilson, and Carlson (1982) that the dark cloud B5, near IC 348 and probably at about the same distance as B205, B1, and B4, is connected with the Taurus nebulae and hence is at about 160 pc. For these reasons we regard the Taurus clouds as foreground, and adopt 350 pc as the distance of NGC 1333.

The proper motions of Fig. 2 are not inconsistent with

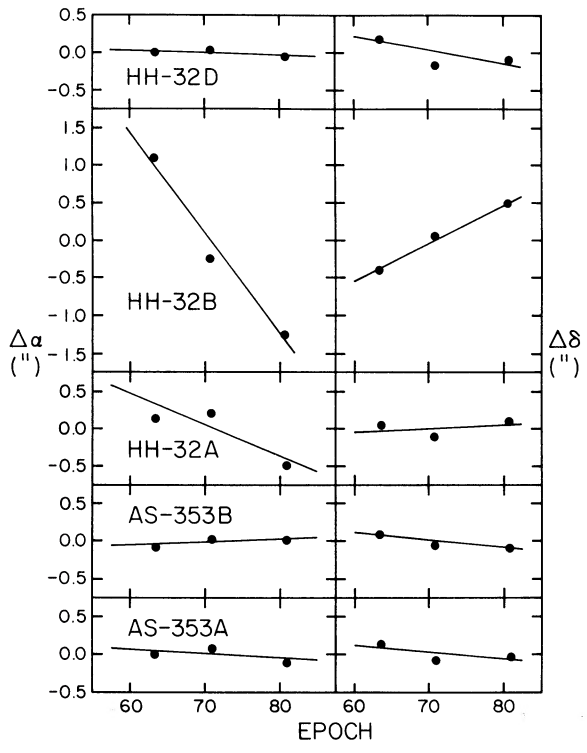

FIG. 3. The position changes for the knots of HH-32 and for AS-353A, B as a function of time. The left panels are right ascension and the right panels declination. The straight lines are the least-squares proper motion fit to the data.

this distance. We used stars dynamically associated with the cloud as our reference frame, and thus their mean motion is zero in our system. In fact, these stars will have some proper motion in a fundamental frame due to their own space velocity as well as to the effects of reflex solar motion. At a distance of 350 pc the reflex solar motion would give them a proper motion of 1".1 cent^{-1} in p.a. 145°. This effect alone would place the absolute zero of proper motion at the position (− 0.9, 0.6) of the cross in Fig. 2, near, but beyond, the centroid of the distribution of the background stars (− 0.7, 0.5). This is what is expected since the mean proper motion of the background stars will also be offset from absolute zero because of the reflex solar motion.

There are numerous emission-Hα stars in the area. Identifications and brief descriptions appear in Herbig and Rao (1972), Herbig (1974), and Liu, Zhang, and Kimura (1980). Several of the brighter of these stars were detected in the near-infrared survey of Turnshek, Turnshek, and Craine (1980).

b) AS-353 and HH-32

The complex of dark lanes and streamers, covering an area of about 40′ × 55′, with which AS-353 is associated is L673. Direct photographs, especially the red Palomar Atlas plate, leave no doubt but that L673 is foreground with respect to the very extensive Aquila obscuration. Weaver's (1949) study of that cloud was centered on a field 4° southwest of L673. He concluded that the Aquila obscuration sets in at about 110 pc and continues out to at least 1 kpc, at which $A_V = 2.6$ mag. The more recent but more fragmentary data compiled by Neckel and Klare (1980) suggest that the extinction in this region has risen to about $A_V = 3$ mag at 3 kpc. Unfortunately, all this yields only a poorly defined upper limit to the distance of L673, and there are no bright normal stars associated with the cloud to provide a spectroscopic value.

The distance may be estimated from the mean proper motion and dispersion in proper motion of stars projected on the cloud. We assume that the obscuration is such that we see no background stars through it. We then observe stars in a cone, the height of which is the distance to the cloud, the base the area of the obscuration. Because of the velocities of the stars and the solar motion, these stars will show some dispersion in proper motion. If the distance to the obscuration is D and the stars velocity dispersion is σ_v, then,

$$\langle \mu^2 \rangle^{1/2} = \sqrt{3}\,(\sigma_V^2 + \tfrac{1}{4}V_s^2)/4.738\ D, \qquad (1)$$

where $\langle \mu^2 \rangle^{1/2}$ is the expected proper motion dispersion in one component and V_s is the component of the solar motion projected onto the axis considered. ($V_s = V_0$ sinλ cos θ, where V_0 is the solar motion, λ is the angular distance from the solar apex, and θ is the angle the direction to the solar antapex makes with the axis under consideration.) Note that Eq. (1) does not depend on having the proper motions in any well-defined system. Equation (1) can be used to find the distance by using the observed proper motion dispersions.

Using the observed equatorial proper motions, we computed the proper motion in galactic longitude and latitude for 12 stars projected upon the cloud containing AS-353A and B. Since HH-32 has a low galactic latitude ($l = 46°$, $b = -1°$), the proper motions in latitude reflect the motions perpendicular to the galactic plane, while those in longitude represent the motions in the plane. We used a value of 19 km s^{-1} for the velocity dispersion perpendicular to the plane (Delhaye 1965). For the dispersion in the plane we took the value $\sigma_p = \{[33 \sin l]^2 + [20 \cos l]^2\}^{1/2}$, where 33 km s^{-1} and 20 km s^{-1} are the velocity dispersions in the direction toward the galactic center and in the direction of galactic rotation, respectively, and l is the galactic longitude of the region (Delhaye 1965). Using these values for the velocity dispersions, we obtained values for the distance of 570 pc using the longitude dispersions and 430 from the latitude.

We can obtain the distance in another manner by looking at the mean proper motion of the stars in the direction of the reflex solar motion. For stars observed in a cone to a limiting distance D, the expected mean proper motion will be

$$\langle \mu \rangle = 3V_s/(2 \cdot 4.738D). \qquad (2)$$

To apply this method to find the distance requires that the proper motions be on a well-defined system. If the reference frame is composed mainly of stars associated with the cloud, this method can give incorrect results. In the case of AS-353A and B and HH-32, the reference frame is composed mainly of stars behind the cloud, with small expected proper motion. This method gives a distance of 280 pc, which is an upper limit because the reference stars themselves are projected upon the more distant Aquila cloud.

As a check on these methods involving the proper motions, we applied them to the region of HH-1 and -2 and to the region of NGC 2068, both part of the Orion complex and known to be at a distance of 470 pc. For HH-1 and -2 we obtained distances of 490 pc, 604 pc, and 633 pc using the dispersions in galactic longitude, latitude, and the mean motion, respectively. In this case, using the mean motion surely overestimates the distance because the reference frame is defined to a large extent by Orion association members. In the case of NGC 2068 we obtained distances of 672 pc, 602 pc, and 529 pc, respectively.

On the basis of all the evidence available to us, including the indication that these astrometric methods tend to overestimate the distance, we adopt the rather uncertain value of 300 pc for the distance of L673.

IV. HH-7 THROUGH -11 AND OTHERS

The proper-motion vectors of HH-7, -8, -10, and -11 are shown together with their 1σ error boxes in the lower half of Fig. 4, below a direct photograph of the area to

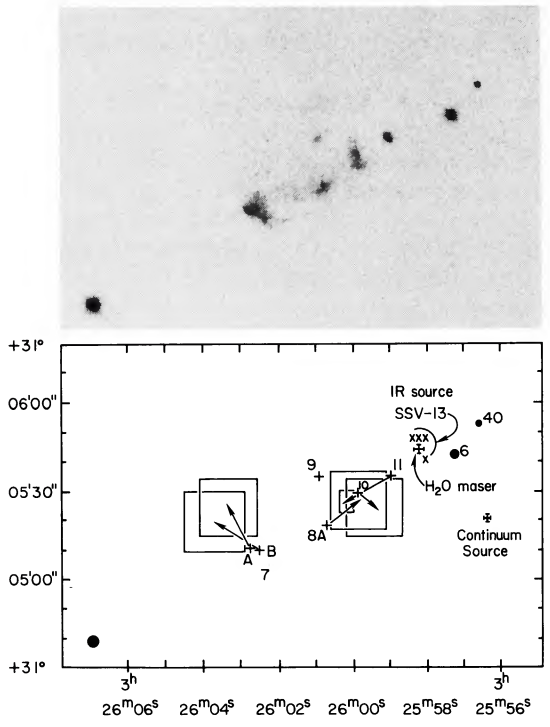

FIG. 4. Above: direct photograph, from a 120-in. red exposure, of the region of HH-7 through -11. Below: a plot, to the same scale, of proper motion vectors (with their 1σ error boxes); the length of the arrows corresponds to the motions in the next 500 years. To minimize congestion, HH-11A is not plotted. The H_2O maser source A is shown at the position given by Haschick *et al.* (1980), while the crosses near it are at coordinates of the infrared source SSV-13 as measured by various observers: Olofsson (1981), Moorwood and Salinari (1983), Cohen and Schwartz (1983), and Simon and Joyce (1983). The 6-cm continuum source is also at the position given by Haschick *et al.*

the same scale. Only HH-11, the smallest and most symmetric of the four Objects, has a cross motion well above the measurement errors. The larger uncertainties for HH-7, -8, and -10 are a consequence of their more extended and complex shapes. Also plotted in Fig. 4 are four determinations of the position of the point source* SSV-13 (Strom, Vrba, and Strom 1976) reported by various infrared observers. The discovery position of Strom *et al.* (1974) is not shown since it is less accurate than the later determinations. These coordinates cluster so convincingly around the radio position of the H_2O maser HH-7-11(A), so named by Haschick *et al.* (1980), that one must conclude that the two sources are the same, to within the uncertainty of present information. This same conclusion has been reached by several earlier investigators. The proper motion vector of HH-11 extends from the direction of SSV-13 (Fig. 4), so it is reasonable to assume that that star is responsible for the motion.

SSV-13 is undetectable on our deepest red plates or spectrograms. This is consistent with its infrared colors as measured by Strom *et al.* (1976) and by Cohen and Schwartz (1983). If one assumes that the intrinsic colors of SSV-13 from 3.5 μm shortward are those of a normal K7 V star (Johnson 1966) and that the extinction curve B of Whittet *et al.* (1976) is applicable, then the photometry of Cohen and Schwartz leads to $A_V = 26$ mag and a predicted apparent magnitude at 0.70 μm of $R = 27$, which would explain the optical invisibility of the star. We place no great weight upon these specific numbers. The questions of the appropriate reddening law aside, if (for example) it had been assumed that the normal colors of SSV-13 were those of a T Tauri star of similar spectral type having an infrared excess (as AS-205), then a comparison of the 1.2-, 3.5-μm colors leads to A_V of only about 18 mag for SSV-13.

SSV-13 is very nearly at the waist of the double-lobed CO structure found by Snell and Edwards (1981), while the negative velocity CO lobe encloses HH-7 through -11. This line of H-H Objects along the symmetry axis of this structure, with the smallest (HH-11) nearest SSV-13 and the largest (HH-7) most distant, hints at a sequence of increasing age, and hence at a series of episodes in the activity of this star. This idea has also occurred to others, for instance Cohen (1982). The average angular spacing between these Objects together with the cross motion of HH-11 provides an estimate of the minimum average time between such hypothetical outbursts, about 500 years. This is a lower bound because HH-11 is at the present time the fastest moving of the group, as evidenced by its much larger radial velocity with respect to the molecular cloud (-146 ± 17 km s^{-1} according to Strom *et al.* 1974) than the other three Objects for which velocities have been measured (which range from -29 ± 15 to -58 ± 14 km s^{-1}).

The angle between the line of sight and the space velocity vector of HH-11A, γ, is in principle specified by the ratio of the radial and angular velocities. The former is -146 km s^{-1}, while the latter is 3".5 cent^{-1}, or 58 km s^{-1} at 350 pc, referred to the mean motion of stars thought to be associated with the cloud. Thus $\gamma = 158°$.

No H-H Objects are known within the area of the positive CO lobe. We have assured ourselves of their absence by reexamining the best deep 120-in. red exposure and the slitless spectrograms on which these Objects were originally established as such. The conventional explanation would be that any Objects propelled in that direction from SSV-13 would lie deeper in the molecular cloud and hence would be more heavily obscured. Yet this explanation, with its assumption that there has been ejection by the star in two opposite directions as is seen at HH-1 and -2 (Herbig and Jones 1981) and at HH-46 and -47 (Graham and Elias 1982; Dopita, Schwartz, and Evans 1982; Graham and Elias 1983) requires that a very high dust opacity overlie the positive lobe. That is, the absence of a detectable counterpart to HH-11 at a similar angular distance (13" or about 0.02 pc) northwest of SSV-13 requires that the visual extinction A_V increases by at least 4 mag over a distance of

*We use the abbreviation SSV rather than the initials in the order that the author's names occurred in their paper because the designation SVS has been pre-empted.

0.02/tan γ pc in the line of sight. Such a value of the specific opacity, ~ 70 mag pc^{-1}, is much higher than that of a cloud in Taurus modelled by Myers 1982 (~ 4 mag pc^{-1}), but only about twice that of the typical small, visually opaque cloud studied by Myers, Linke, and Benson 1983 (~ 35 mag pc^{-1}). Thus the existence of such a highly opaque region is not unreasonable; what is puzzling is how such a high density could have survived in that volume in the face of a CO outflow that should have cleared it of dust, an outflow that would be required to explain the hypothetical H-H Object. This contradiction inclines us to suspect that, as at R Mon (Jones and Herbig 1982), no such counter-Objects exist in the positive lobe: i.e., that SSV-13 has for some reason only driven H-H Objects in the one direction. We assume, obviously, that the heavy extinction of SSV-13 itself is produced in its immediate vicinity. A consequence of this idea is that the value of γ corresponds to our viewing the star from about latitude 68° (the polar direction being defined by the motion of HH-11). This shows that the circumstellar material around SSV-13 is not in the form of a thin disk: it must be arranged as a very thick torus, but thin enough at one pole to permit the propulsion of HH-11.

It should be mentioned that there is a line of four faint stars extending to the west of SSV-13 that is curiously similar to the alignment of HH-7 through -11 in nearly the opposite direction. The proper motions of these stars have been measured; they are all very small, quite unlike the motion of HH-11. All show continuous spectra on the 1956 slitless spectrograms, with no obvious Hα emission. Star 39, the one nearest SSV-13, "varied significantly" in 1974 according to van den Bergh (1975). Nevertheless, we see no reason to regard this alignment as any more than an accident, or to associate any of these stars with the activity of SSV-13.

HH-4 and -17 are very faint, extended surfaces, each having a faint star or sharp nucleus near one edge. It is these nuclei that were measured. Neither showed motion above the level of the measurement errors. HH-5 is a small, bright bar-like Object. The point of peak intensity near the southwest end of the bar was measured.

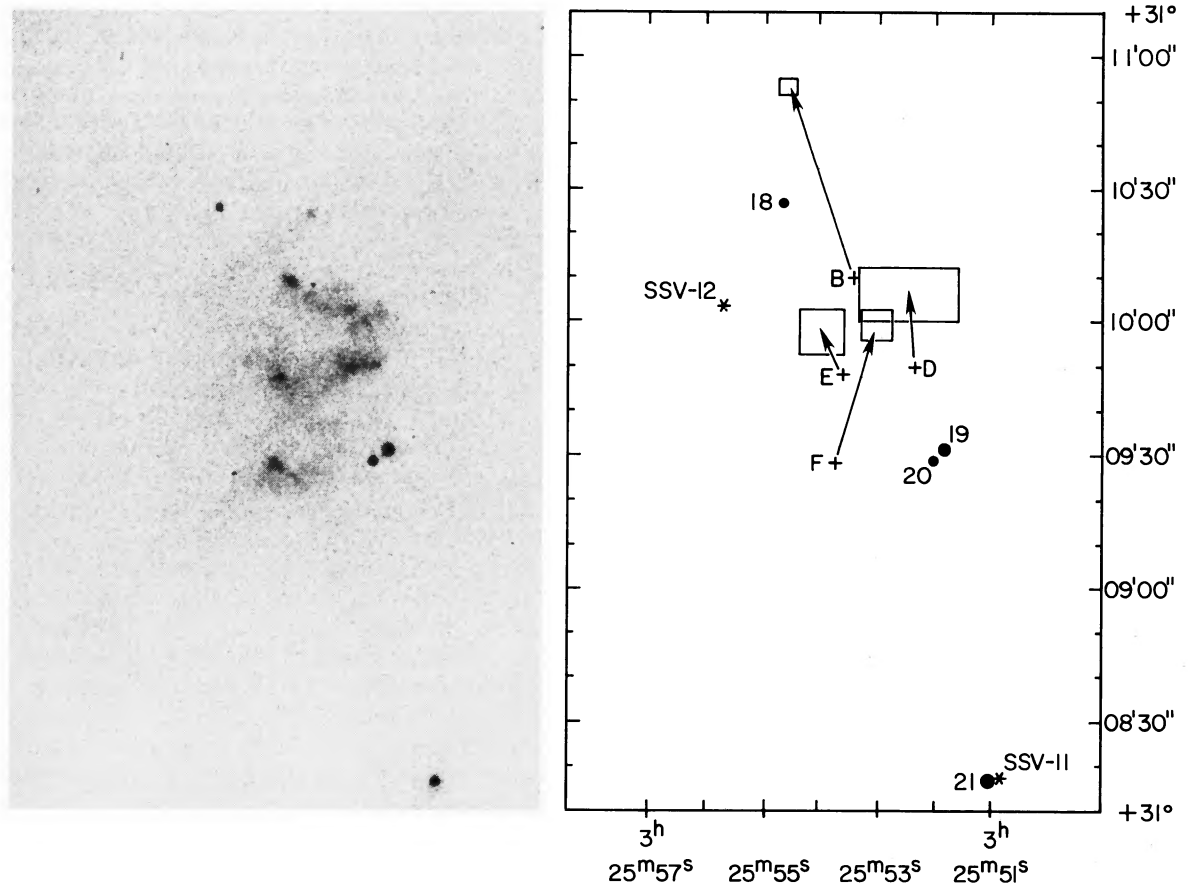

FIG. 5. Direct photograph (left) and proper motion vectors (right) for the main nuclei of HH-12. The arrow lengths correspond to the motions in the next 300 years, and their 1σ error bars. The infrared sources SSV-11 and -12 are shown at the coordinates given by Cohen and Schwartz (1983), while all the stars are plotted at their optical positions.

Again, no significant motion was found.

V. HH-12

HH-12 is an intricate mass of condensations superimposed upon more amorphous nebulosity (Fig. 5); the whole structure has dimensions of about $45'' \times 65''$. Four of the brighter condensations are measurable and show proper motions that are well in excess of their uncertainties (Fig. 5). Several infrared sources in the neighborhood were found by Strom *et al.* (1976), and have been remeasured by Cohen and Schwartz (1983). The one of these which is most nearly aligned with the reversed proper motion vectors of HH-12 is SSV-11, about 95″ to the south. Its coordinates by Cohen and Schwartz agree to well within their uncertainty with the optical position of star 21, a faint ($R = 17$) feebly nebulous star. Star 21 was consistently suspected to have Hα in emission on the original slitless spectrograms of the field. This suspicion has been confirmed by a low-resolution (7-Å) IDS scan very kindly obtained for us, through the courtesy of Dr. R. P. Kraft, by Ms. E. Friel with the 120-in. Cassegrain scanner on 1982 September 30. That observation shows star 21 to have rather strong Hα emission, although no other emission lines are present. The features of a late-type stellar spectrum are visible, and comparison with a set of scans of dwarf standards (kindly provided by Dr. S. Faber) indicates a type near M1.

Obviously, SSV-11 is not so heavily obscured as is SSV-13. The photometry of Cohen and Schwartz (1983), if the energy distribution is that of a normal M1 V (Johnson 1966), leads to $A_V = 8.8$ mag and a predicted R (0.7 μm) = 17.7, which cannot be far from the truth, although no visual region photometry of SSV-11 is available. The infrared photometry, if extrapolated still further, leads to $V_0 = 12.8$. At 350 pc this corresponds to $M_V = +5.1$, which would locate star 21 = SSV-11 about 4 mag above the main sequence at M1. Note, however, that these figures depend upon the assumption of a normal reddening law.

The original slitless spectrograms of the region, obtained in 1956, were not calibrated so one can say only that the Hα emission in star 21 at that time was weak. A photometrically standardized investigation of other such plates taken with the same equipment by Marcy (1980) indicates that this generally corresponds to a Hα equivalent width of 5–20 Å. The IDS scan, however, shows that Hα in 1982 had $W_\lambda = 65$ Å, a difference too large to be explained by the uncertainty of either observation. Van den Bergh (1975) noted that star 21 had varied in magnitude between two plates taken three months apart in 1974. We have available 10 Crossley and 120-in. red direct plates of the field (Table I) on which iris photometer settings were recorded as part of the measuring procedure with the AME. These settings cannot yet be converted into magnitudes for lack of faint standards in the area, but we have examined the scatter of the individual iris readings for some 58 faint stars in the field. One of the five known Hα-emission stars examined (LkHα-353) stands out with a conspicuously large dispersion, but the others do not, and star 21 shows only a slightly larger scatter than the bulk of presumably constant nonemission stars in the area. Therefore the evidence for photometric activity in star 21 is marginal, but from the nature of the spectrum, which is like that of many T Tauri stars observed at that resolution, it would not be surprising if the star is variable in both spectrum and light.*

As for HH-11, the angle that the velocity vector of HH-12 makes with our line of sight can be estimated. The only published radial velocity is that by Strom *et al.* (1974), -65 ± 3 km s^{-1}, with respect to the molecular cloud, for an unspecified condensation. If this is combined with the best determined cross motion in HH-12 of $15''.2 \pm 0''.9$ cent^{-1} for condensation B, then $\gamma \approx 104°$. If the mean motion of nuclei E, D, and F is used instead ($6''.6$ cent^{-1}), then $\gamma \approx 121°$. In either case, there is a conspicuous difference between the resulting pictures of SSV-11 and SSV-13. SSV-13 at HH-7 through -11 is viewed from a high latitude (68°), but has a much larger extinction ($A_V \approx 20$–25 mag?) than SSV-11, which is seen from a lower latitude (14° or 31°), yet has only $A_V \approx 9$ mag. There are several ways, short of abandoning the conventional model of an equatorial disk or torus about the stars, that this difference might be explained. (a) The measured cross motions do not represent material motion in the same sense as do the Doppler shifts, or are in some way distorted by photocenter changes. (b) The disk at SSV-13 is younger and hence denser than at SSV-11. This idea might be supported by the fact that repeated ejection has taken place at SSV-13 at intervals of about 500 years (Sec. III), while only one event is apparent at SSV-11, which took place either 800 or 1400 years ago depending upon the cross motion adopted for HH-12. It is our intention to redetermine the radial velocities of these Objects before taking a position on such speculations.

VI. HH-32

a) The Spectrum of AS-353A

The bright Hα line in AS-353A† was discovered independently by Merrill and Burwell (1950) and by Iriarte and Chavira (1956). Apparently, the first slit spectro-

*S. E. Strom has suggested (private communication 1983) that the faint star (No. 7 in Table III) about 37″ southeast of No. 21 may instead be the exciting star of HH-12. The image of this star is indeed crossed by a streak of faint nebulosity that extends in the direction of HH-12. But unlike 21, star 7 was not detected in the infrared surveys, nor is Hα emission apparent on our slitless spectrograms, nor do the iris photometer residuals (in either case) indicate variability. The proper motions of both stars are very small, and thus both may be associated with the cloud. The well-determined velocity vector of HH-12B (Fig. 5) definitely points backward toward 21 rather than 7, but the less certain vector of HH-12F favors star 7. Our opinion is that none of this evidence is convincing, but on balance the available evidence seems to favor star 21 as the propellant of HH-12.

†AS-353A = Ir-Ch 34 is also V1352 Aql. A variation in the combined V light of A and B of about 0.7 mag over 470 days was found by Kopatskaya and Shulov (1978). Their mean values are: $V = 12.46$, $B - V = +1.05$.

scopic observations were two 100 Å mm^{-1} spectrograms of the 3500–5000 Å region obtained by Herbig in 1964. Higher-resolution observations, mostly in the red, were made at Lick in 1974 and subsequently, and new observations have recently been reported by Mundt, Stocke, and Stockman (1982). In the photographic region, AS-353A shows a strong, smooth continuous spectrum with an intense display of Ca II, Fe II, and Ti II emission lines, plus weaker lines of Fe I and Ca I. The Hα line is very strong and wide, and is cut shortward of its peak by a deep absorption component beyond which the emission wing reappears. It is therefore an example of Beals' Type III profile, not the classical P Cyg (Type I) in which no emission is present beyond the absorption. Down the series beyond Hβ, this absorption component increasingly dominates the Balmer profile so that from H8 to H13, only a deep, sharp shell-type absorption line is seen. Similar narrow absorptions of Ti II $\lambda\lambda$ 3685, 3759, 3761 are present, as in many conventional shell spectra. The presence of an overlying cooler layer is apparent also at Ca II λ 3968, whose emission is obliterated by the displaced Hϵ absorption while Ca II λ 3933 remains strong in emission. Further demonstration that the emission region lies below the shell is provided by the presence of the fluorescent Fe I lines $\lambda\lambda$ 4063, 4132, characteristic of T Tauri stars. These lines are excited selectively through the near coincidence of Fe I λ 3969 with Ca II λ 3968 or Hϵ, but obviously that would be impossible if the radiation field were that which we see from the outside of the shell. No normal stellar absorption spectrum is present on the Lick plates.

The absorption spectrum seen in AS-353A is clearly that of a detached layer rising with respect to the star. Consequently we regard the displacement of the absorption line minima as indicative of the shell velocity, rather than that of the shortward edges, as in the case of conventional P Cyg structure. The two 1964 spectrograms, obtained a week apart, give mean velocities of -99 and -94 km s^{-1} for the shell lines measured between Hβ and H13. Ten years later, a plate of the red region gave for Hα -165 and for the Na I D lines -165 km s^{-1} and, three months later, -196 and -188 km s^{-1} for these same lines. Scans published by Mundt, Stocke, and Stockman (1982) indicate displacements (for the line centers) of about -194 km s^{-1} for both lines in 1982. There is thus some indication, from the one Lick spectrogram, of a small change in the shell velocity from Hα and Na I. But whether the large discrepancy between the higher Balmer lines measured in 1964 and the red lines in 1974–82 represents a major change in the star over that decade, or a "Balmer progression" as is often seen in shell spectra, awaits simultaneous observation of both spectral regions.

b) The Motion and Spectrum of HH-32

HH-32A is a very small (about 3″ across), roughly triangular nebulosity that is 22.″8 in p.a. 288° from AS-353A. HH-32B is a much fainter, fuzzy spot 7.″2 in 133° from HH-32A. Both A and B are found to have large cross motions directed away from AS-353AB. The velocity vectors are approximately parallel, but quite different in magnitude. They are shown in Fig. 6 as motions over 500 years. At 300 pc, these motions correspond to 54 km s^{-1} (HH-32A) and 202 km s^{-1} (HH-32B) with respect to the zero point of our proper motion system. In contrast, the motions of AS-353A and B are so small as to lie within their 1σ error boxes of about 14×14 km s^{-1}.

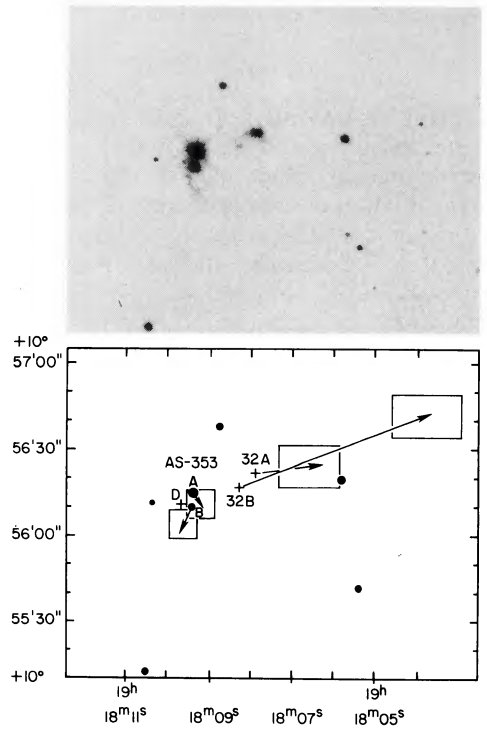

FIG. 6. Direct photograph (above) and proper motion vectors (below) for AS-353A, B, and HH-32A, B. The arrow lengths show the motions in the next 500 years, and their 1σ error boxes.

The spectrum of HH-32A is very interesting, and unique among the H-H Objects we have observed so far. Figure 7 shows a 34-Å mm^{-1} coudé image-intensifier spectrogram in which the slit, about 40″ long, passed through AS-353A (the overexposed streak near the top) and HH-32A. The Hα, [N II], [O I], and probably the [S II] emission lines of HH-32A are double. The stronger and sharper component has a heliocentric velocity of $+20 \pm 4$ km s^{-1} (mean value from three 34 and 11 Å mm^{-1} spectrograms), while the wider and weaker is at $+208 \pm 11$ km s^{-1}. This line splitting was discovered independently by Dopita (1978), who gave velocities of $+2 \pm 15$ and $+296 \pm 15$ km s^{-1}. Mundt *et al.* obtained $+62$ and $+225$ km s^{-1}. The greater width of the longward component is striking on the 11-Å mm^{-1} plates: the wings of the stronger lines fade into the background at about 80 km s^{-1} either side of the line center.

A quantitative measure of these lineswidths was ob-

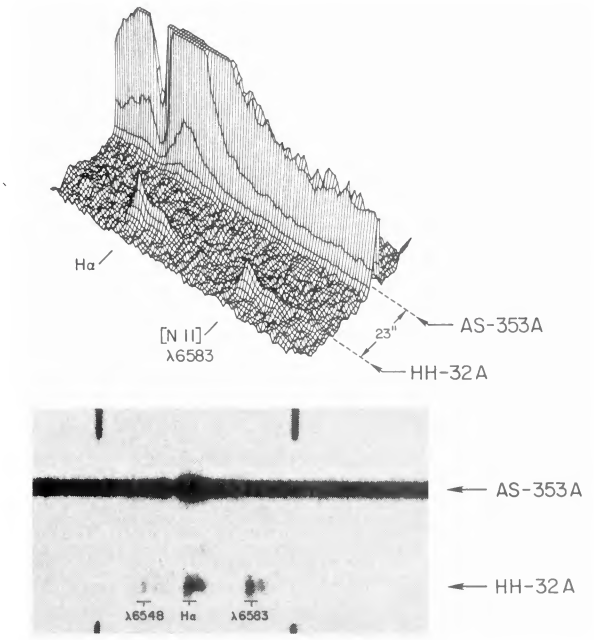

FIG. 7. Above: perspective intensity plot of the Hα, λ 6583 region of AS-353A and HH-32A, from the spectrogram shown below. The duplicity of the lines of HH-32A is apparent. The original dispersion was 34 Å mm^{-1}, with slit in p.a. 105°. The spectrogram (below) shows not only the line doubling but also the slight displacement of the weaker (wider) components toward the star.

tained by fitting Gaussians to direct-intensity scans of the best 11-Å mm^{-1} plate, made with a nearly point microphotometer slit. The results for the half-width at half peak intensity (not the Gaussian σ) of the two components of Hα were 44 ± 3 and 80 ± 5 km s^{-1}, after a small correction for instrumental resolution. The same quantities for [N II] λ 6583 were 48 ± 3 and 78 ± 7 km s^{-1}. The uncertainties quoted come only from the internal agreement of the individual microphotometer scans.

Furthermore, all these unwidened coudé spectrograms show that the photocenter of HH-32A in the narrow set of lines at + 20 km s^{-1} is slightly displaced along the slit (i.e., along the line connecting HH-32A and AS-353A) with respect to the center defined by the + 208 km s^{-1} component. This offset of the two spectra is apparent in Fig. 7. The mean displacement from three spectrograms is 0".42 ± 0".03, in the sense that the narrow, + 20 km s^{-1} spectrum is the more distant from AS-353A in the direction of p.a. 285°, the slit orientation for these plates.

We ourselves have only a low-dispersion spectrogram of HH-32B, but the observations of Mundt *et al.* show that its velocity is large and positive. They obtained a value of + 260 km s^{-1} for the peak of Hα; their published profile suggests that a wing or another weaker line is also present at lesser velocity. This is rather similar to what we observe at HH-32A except that the relative intensities are reversed. Thus both HH-32A and B are unusual among H-H Objects in their possession of large positive velocities. Both their position with respect to AS-353A and the orientation of their proper motion vectors are in the direction of an extension of the positive-velocity CO region around AS-353 mapped by Edwards and Snell (1982). The obvious interpretation is that both Objects are being driven away from us, into the cloud, by a wind from AS-353A and that they are detectable because that wind has removed the dust in our line of sight. Brugel, Böhm, and Mannery (1981) have derived the relatively small value of $E(B-V) = 0.69$ for HH-32A from its [S II] emission-line ratios. [The extinction of AS-353A itself is undetermined because the normal color of such a peculiar star is unknown, but Cohen and Kuhi (1979) have estimated that $E(B-V) = 0.94 \pm 0.1$ from the colors of AS-353B, of type M0.] It is reasonable to assume that the wind which drives HH-32B is the same shell we see projected upon AS-353A. The velocity of that material is about − 185 km s^{-1} with respect to the molecular cloud, and one might presume it reaches HH-32AB with the same velocity, a presumption which we shall question.

The explanation of the double emission lines in HH-32A is not so obvious. We offer the following conjecture: that the broad lines at + 218 km s^{-1} (with respect to cloud) originate in the pre-shock material arriving near HH-32A directly from AS-353A, but at that star's *polar* wind velocity, while the narrow-lined spectrum at + 30 km s^{-1} is formed in post-shock gas nearer HH-32A. The H-H Object is thus supposed to be a slowly moving obstacle against which the wind impinges. This sequence of locations is suggested by the offset of the two sets of lines in HH-32A, the sharper set at lower velocity being the more distant from AS-353A. The geometry is suggested in Fig. 8. The angle γ, as in Secs. III and IV, is

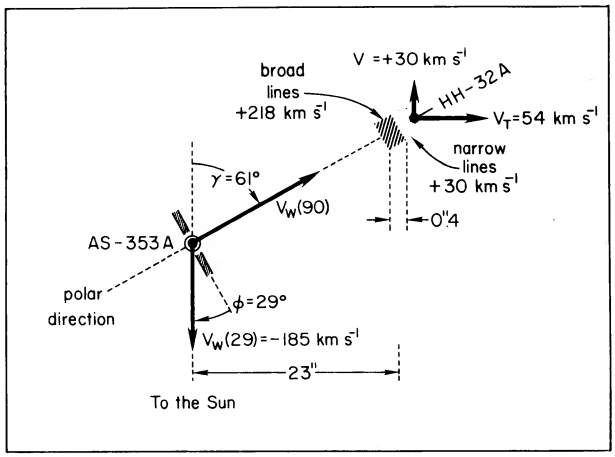

FIG. 8. Schematic geometry of the model of HH-32A being driven by the wind from AS-353A, as described in the text. The heavy arrows are velocity vectors. The shaded bar at AS-353A indicates the orientation of the circumstellar disk. The $V_w(\phi)$'s indicate the wind velocity from the star toward latitude ϕ, while V_T and V are the tangential and radial velocities of HH-32A with respect to the cloud.

between the line of sight and the velocity vector of HH-32A. We assume that the velocity of the narrow line is approximately that of HH-32A itself; combined with the tangential velocity, it yields $\gamma = 61°$. The stellar wind arriving at HH-32A will therefore be observed to have a radial velocity as seen from Earth of $V_w(90)\cos\gamma$, where $V_w(90)$ is the velocity of the polar wind that departs the star at latitude 90°. We have observed at AS-353A that $V_w(29) = 185$ km s^{-1}. It has been shown (Jones and Herbig 1982) that at R Mon, a somewhat similar pre-main-sequence star, that there is a strong dependence of V_w upon latitude such that in that case $V_w(90)/V_w(29) \approx 3$. If this factor were applicable to AS-353A, we would expect to see a radial velocity of about $+270$ km s^{-1} for the wind arriving at HH-32A, as compared to the $+218$ km s^{-1} observed. We place no importance on the magnitude of the discrepancy, only on the sense of the prediction, because the conditions at R Mon may very well not apply at AS-353A. The point is that a not unreasonable geometrical arrangement and choice of parameters could account for the velocity of the broad-line spectrum of HH-32A.

An opposing view could be that the line splitting represents real relative motion of two nearly superimposed regions within HH-32A. The radial velocity difference of 188 km s^{-1} corresponds to a relative tangential velocity of 339 km s^{-1} if $\gamma = 61°$. At 300 pc, this would imply an angular movement of one region with respect to another of 0".24 yr^{-1}. Since the angular offset was 0".4 on the 1977 spectrograms, this would require that an elongation of the image of about 4" at the time of the first 120-in. direct plate (in 1963) would have shrunk to nearly zero about 1979. Although some small variation in the image structure is suspected, no such progressive change in size or shape can be seen on the 120-in. plates. Thus we find no support for this idea. It might be mentioned that a similar case of line doubling is observed in HL Tauri, but again, no obvious change in the image of that star has been observed.

Another view might be that the split lines of HH-32A represent the orbital motion of a double-line spectroscopic binary. The angular separation and relative velocity suggest an orbital period of about 20 years. This view cannot be challenged on the grounds that no major change in the line structure has been observed, because high-resolution spectroscopy has been carried out only over the past five years. However, the total mass of the binary that is implied by this period and separation is about 4500 solar masses, which we do feel is enough to reject the hypothesis.

A natural question is whether these two regions of HH-32A could be identified with the two density domains that Böhm and his collaborators have introduced in their modelling of the spectra of H-H Objects. In the case of HH-32A, Brugel, Böhm, and Mannery (1981) have represented the integrated spectrum with a high-density region ($n_e = 2.5\times10^4$ cm^{-3}) having a small filling factor of about 10^{-3}, plus a low-density region ($n_e = 1\times10^3$ cm^{-3}), both at $T_e = 10\,100$ K. Their model predicts that the high-density volume contributes from 32% to 66% of the total flux in the [O I], [N II], and [S II] lines; i.e., that in these lines, the two regions contribute about equally.

Our measured values of the flux ratios (in the sense shortward/longward component) of the stronger emission lines in HH-32A are given in the upper line of Table V. The lower line gives the expected ratio (from Gomez 1981) if the two components originate, respectively, in the high- and low-density regions of the Brugel *et al.* model. There is reasonable correspondence for [O I] and [N II], but critical comparison should be with the density-dependent [S II] lines, although our ratios for $\lambda\lambda$ 6716, 6730 are very uncertain because the longward component is very weak. If the two components in the spectrum do represent the two density domains of the model, then the two components of λ 6730 ought to be of nearly equal intensity, which is certainly not observed, and the ratio for λ 6716 would be reversed. Better spectroscopic observations are urgently needed, but clearly, our present data do not support this idea.

Why should HH-32A (and possibly HH-32B also) be the only conventional H-H Objects to show such a clear case of line doubling? It is tempting to speculate that this is because of an unusual and favorable aspect angle: the positive radial velocity means that we see HH-32A from the side that it is impacted by the wind from AS-353A, while in H-H Objects having negative velocities the wind strikes the far side and thus the Objects itself may to some degree block our view of arriving gas. In such a case, one would therefore expect the arriving material to have a large negative velocity. Several of the condensations in the Orion Nebula described by Cantó, Goudis, Johnson, and Meaburn (1980) and by Axon and Taylor (1983) show extended negative-velocity wings on the

TABLE V. Observed and expected line ratios in HH-32A.

Ion Line	[O I] λ 6300	Hα 6563	[N II] 6583	[S II] 6716	[SII] 6730
Observed flux ratio (shortward/longward component)	2.2	1.1	1.5	2.4:	1.8:
Expected flux ratio (high density/low density component)	1.94	—	1.56	0.47	1.08

[S II] and [O I] lines that may be imperfectly resolved structures of this kind. No line splitting would be expected in Objects having small radial velocities because even if the impacted side were partially visible, there would be only a small Doppler component and the two spectra would be superimposed.

It is obvious that our discussion of HH-32A as if it were a slow-moving obstruction in the high-velocity wind of AS-353A is more compatible with the interpretation of H-H Objects urged by Schwartz and Dopita (1980) than with the "interstellar bullet" hypothesis of Norman and Silk (1979).

c) Other Nebulosity near AS-353

Mundt *et al.* have discussed the possible significance of a very faint area of emission nebulosity that they discovered on deep CCD exposures about 10″ southeast of AS-353A (and named HH-32C), and for which they obtain a radial velocity from Hα of about -18 km s^{-1}. This nebulosity is not detectable with certainty on our 120-in. direct plates, but they do not go so faint as do the Steward CCD images. One coudé spectrogram does show a faint Hα emission line that extends to about 15″ (p.a. 107°) from AS-353A, and which has a velocity of -50 km s^{-1}. We presume this is HH-32C. There is thus some support to the belief of Mundt *et al.* that the radial velocities change sign at AS-353A. A similar but much clearer situation has been found at HH-46, -47 (Graham and Elias 1982; Dopita, Schwartz, and Evans 1982; Graham and Elias 1983).

The 120-in. direct plates show a sharp point-like image at 6.″0 in 134° from AS-353A. It was measured for proper motion in the chance that it might be a H-H Objects. Any motion is, however, below the measurement uncertainty (Table III); it is probably a star.

VII. CONCLUSIONS

(1) The well-determined proper motion of HH-11 is directed away from the heavily obscured star SSV-13, which is also a H_2O maser source; the minimum travel time inferred from the cross motion of HH-11 is about 400 years. The images of the nearby HH-7, -8, and -10 are too poorly defined for reliable measurement, except that none seems to be extremely large. Their arrangement in a chain on the sky, in order of increasing angular size with distance from SSV-13, hints that they may be the result of repetitive ejection from the vicinity of the star at intervals $\gtrsim 500$ years. All these Objects lie in the negative-velocity lobe of the CO structure centered at SSV-13. None is detectable in the positive lobe. It is argued that this absence is real: that the star has in the recent past propelled H-H Objects only in the one direction.

(2) Four measurable condensations in the extended Objects HH-12 show, fairly convincingly, movement away from the moderately reddened and possibly variable Mleα star SSV-11. Thus, although the HH-7 through -11 group and HH-12 are only 4.′5 apart, they are driven by different sources. HH-12, with a travel time of 800–1400 years, is the only artifact of such activity at SSV-11 while there are five such objects at SSV-13. Therefore the latter, the more heavily obscured, could be the younger and more active star. Again, there are no detectable H-H Objects on the opposite side of SSV-11.

(3) The motions of HH-32A and -32B are directed away from the bright T Tauri-like star AS-353A, although by different amounts. The spectrum of HH-32A is unusual in its display of two sets of emission lines, both having positive velocities with respect to the cloud: the narrower at $+30$ km s^{-1} and the wider at $+218$ km s^{-1}. The photocenter of HH-32A in the $+30$ km s^{-1} spectrum is slightly (0.″4) displaced toward AS-353A with respect to that of the $+218$ km s^{-1} lines. We speculate that these two physically offset spectra represent post- and pre-shock stellar wind gas from AS-353A arriving at an obstruction. The star itself shows a displaced shell spectrum having a velocity of -185 km s^{-1}, which we identify with the same wind. We speculate further that the line duplicity of HH-32A is a consequence of an unusual aspect angle: such positive radial velocities are rare among H-H Objects, and when they do occur, may mean that the observer is then able to see arriving pre-shock material that in the negative-velocity case is hidden by the Object itself.

(4) It has not been possible to identify these two spectra in HH-32A with the two domains of high and low density that Böhm and his collaborators have inferred from analysis of the combined spectrum, to be present in HH-32A.

(5) Some evidence is found in favor of the proposal by Mundt, Stocke, and Stockman that very faint negative-velocity Hα emission exists on the opposite side of AS-353A from HH-32. Unless that faintness is caused by the arrangement of foreground extinction, one would have to conclude that AS-353A is more effective in exciting (or accelerating) H-H Objects in one of its polar directions than in the opposite. In the Schwartz-Dopita picture, this would be because there is less ambient cloud material in the foreground with which the stellar wind can interact than in the background. The Norman-Silk alternative is that there is some asymmetry at the star: for example, that the wind flux from the unobservable farther hemisphere of AS-353A is more effective than that over the near side.

We are indebted to Mr. E. A. Harlan for obtaining some of the Crossley direct plates used in the investigation, Mr. R. Goodrich for preparing the plot of Fig. 7, Ms. E. Friel for obtaining the scan of star 21, and Mr. M. Sirk for helping with the manual measures. We are also grateful to the National Science Foundation for partial support of this investigation under Grants AST 82-03115, AST 80-16989, and AST 81-12347.

REFERENCES

Axon, D. J., and Taylor, K. (1983). Mon. Not. R. Astron. Soc. (in press).

Blaauw, A. (1963). In *Basic Astronomical Data*, edited by K. Aa. Strand (University of Chicago Press), p. 383.

Borgman, J., and Blaauw, A. (1964). Bull. Astron. Inst. Neth. **17**, 358.

Brugel, E. W., Böhm, K. H., and Mannery, E. (1981). Astrophys. J. Suppl. **47**, 117.

Canto, J., Goudis, C., Johnson, P. G., and Meaburn, J. (1980). Astron. Astrophys. **85**, 128.

Cohen, M. (1975). Publ. Astron. Soc. Pac. **87**, 421.

Cohen, M. (1982). Publ. Astron. Soc. Pac. **94**, 266.

Cohen, M., and Kuhi, L. V. (1979). Astrophys. J. Suppl. **41**, 743.

Cohen, M., and Schwartz, R. D. (1983). Preprint.

Delhaye, J. (1965). In *Galactic Structure*, edited by A. Blaauw and Maarten Schmidt (University of Chicago Press), p. 61.

Dopita, M. A. (1978). Astrophys. J. Suppl. **37**, 117.

Dopita, M., Schwartz, R. D., and Evans, I. (1982). Astrophys. J. **263**, L73.

Edwards, S., and Snell, R. L. (1982). Astrophys. J. **261**, 151.

Eichhorn, E., and Jefferies, W. H. (1971). Publ. Leander McCormick Obs. **16**, 267.

Gomez, P. (1981). Quoted by C. Goudis in *The Orion Complex* (Reidel, Dordrecht), p. 276.

Graham, J., and Elias, J. H. (1982). Paper presented at Leiden "Galactic Surveys Workshop," August 1982.

Graham, J., and Elias, J. H. (1983). Astrophys. J. (in press).

Harris, D. L., Morgan, W. W., and Roman, N. G. (1954). Astrophys. J. **119**, 622.

Haschick, A. D., Moran, J. M., Rodriguez, L. F., Burke, B. F., Greenfield, O., and Garcia-Barreto, J. A. (1980). Astrophys. J. **237**, 26.

Herbig, G. H., and Rao, N. K. (1972). Astrophys. J. **174**, 401.

Herbig, G. H. (1974). Lick Obs. Bull. No. 658.

Herbig, G. H., and Jones, B. F. (1981). Astron. J. **86**, 1232.

Iriarte, B., and Chavira, E. (1956). Bol. Obs. Tonantzintla Tacubaya **14**, 31.

Johnson, H. L. (1966). Annu. Rev. Astron. Astrophys. **4**, 193.

Jones, B. F., and Herbig, G. H. (1982). Astron. J. **87**, 1223.

Kopatskaya, K. N., and Shulov, O. S. (1978). Trudy Astron. Obs. Leningrad **34**, 94.

Liu, Cai-pen, Zhang, Chun-sheng, and Kimura, H. (1980). Act. Astron. Sinica **21**, 354; Chin. Astron. Astrophys. **5**, 276.

Marcy, G. W. (1980). Astron. J. **85**, 230.

Merrill, P. W., and Burwell, C. G. (1950). Astrophys. J. **112**, 72.

Moorwood, A. F. M., and Salinari, P. (1981). Astron. Astrophys. **94**, 299.

Mundt, R., Stocke, J., and Stockman, H. S. (1983). Astrophys. J. **265**, L71.

Myers, P. C. (1982). Astrophys. J. **257**, 620.

Myers, P. C., Linke, R. A., and Benson, P. J. (1983). Astrophys. J. **264**, 517.

Neckel, T., and Klare, G. (1980). Astron. Astrophys. Suppl. **42**, 251.

Norman, C. A., and Silk, J. (1979). Astrophys. J. **228**, 197.

Olofsson, H., quoted by Sandell, G., and Olofsson, H. (1981). Astron. Astrophys. **99**, 80.

Schwartz, R. D., and Dopita, M. A. (1980). Astrophys. J. **236**, 543.

Simon, T., and Joyce, R. R. (1983). Astrophys. J. **265**, 864.

Snell, R. L., and Edwards, S. (1981). Astrophys. J. **251**, 103.

Strom, S. E., Grasdalen, G. L., and Strom, K. M. (1974). Astrophys. J. **191**, 111.

Strom, S. E., Vrba, F. J., and Strom, K. M. (1976). Astron. J. **81**, 314.

Turnshek, D. A., Turnshek, D. E., and Craine, E. R. (1980). Astron. J. **85**, 1638.

van den Bergh, S. (1975). Publ. Astron. Soc. Pac. **87**, 405.

Weaver, H. F. (1949) Astrophys. J. **110**, 190.

Whittet, D. C. B., Van Breda, I. G., and Glass, I. S. (1976). Mon. Not. R. Astron. Soc. **177**, 625.

Young, J. S., Goldsmith, P. F., Langer, W. D., Wilson, R. W., and Carlson, E. R. (1982). Astrophys. J. **261**, 513.